Thermogravimetric and model-free kinetic studies on CO_2 gasification of low-quality, high-sulphur Indian coals

Tonkeswar Das, Ananya Saikia, Banashree Mahanta,
Rahul Choudhury and Binoy K Saikia*

Polymer Petroleum and Coal Chemistry Group, Materials Science & Technology Division, CSIR-North East Institute of Science and Technology, Jorhat 785 006, Assam, India.
**Corresponding author. e-mail: bksaikia@rrljorhat.res.in; bksaikia@gmail.com*

Coal gasification with CO_2 has emerged as a cleaner and more efficient way for the production of energy, and it offers the advantages of CO_2 mitigation policies through simultaneous CO_2 sequestration. In the present investigation, a feasibility study on the gasification of three low-quality, high-sulphur coals from the north-eastern region (NER) of India in a CO_2 atmosphere using thermogravimetric analysis (TGA-DTA) has been made in order to have a better understanding of the physical and chemical characteristics in the process of gasification of coal. Model-free kinetics was applied to determine the activation energies (E) and pre-exponential factors (A) of the CO_2 gasification process of the coals. Multivariate non-linear regression analyses were performed to find out the formal mechanisms, kinetic model, and the corresponding kinetic triplets. The results revealed that coal gasification with CO_2 mainly occurs in the temperature range of 800°–1400°C and a maximum of at around 1100°C. The reaction mechanisms responsible for CO_2 gasification of the coals were observed to be of the 'nth order with autocatalysis (CnB)' and 'nth order (Fn) mechanism'. The activation energy of the CO_2 gasification was found to be in the range 129.07–146.81 kJ mol^{-1}.

1. Introduction

Coal is the most abundant fossil fuel on Earth. Coal plays an important and indispensable role in the future energy mix, with a very large resource base and economically recoverable reserves, much greater than those of oil and gas. The usage of coal is continually increasing for power generation in India and is needed to meet the energy demand of steel, cement, and the manufacturing industries (Sahu 2013). Coal-based thermal power plants generate about 60% of the commercial energy needs and 70% of the electrical power in India (Sahu 2013). However, the simultaneous emission of greenhouse gases (GHG) and other pollutants during coal combustion for power generation in the Indian power sectors is one of the major environmental issues (Sinag *et al.* 2003; Irfan *et al.* 2011; Mishra *et al.* 2014; Saha *et al.* 2012; Sahu 2013). Carbon dioxide (CO_2) is considered to be the main source of greenhouse gas emissions which is a major threat to global warming and climate change (Sinag *et al.* 2003; Irfan *et al.* 2011; Mishra *et al.* 2014; Saha *et al.* 2012, 2013). According to the Intergovernmental Panel on Climate Change (IPCC), CO_2 emissions from fossil fuel combustion and industrial processes contributed about 78% of the total GHG emission increase from 1970 to 2010. Fossil fuel-related CO_2 emissions reached 32 (±2.7) Gt CO_2/year in 2010 and grew further by about 3% between 2010 and 2011 and by about 1–2% between 2011 and 2012 (Irfan *et al.* 2011).

Keywords. Low-quality coal; Indian coal; CO_2-gasification; thermogravimetric analysis; model-free kinetics.

J. Earth Syst. Sci., DOI 10.1007/s12040-016-0743-5, **125**, No. 7, October 2016, pp. 1365–1377

Due to some disadvantage of the traditional coal-fired power plants, the zero-emission (clean coal technology coupled with carbon capture and sequestration) power plant for power generation in a nitrogen-free atmosphere, mostly known as oxy-fuel or O_2/CO_2 combustion technology, is one of the new promising methods (Zhigang *et al.* 2013). Recently, coal gasification with CO_2 and oxygen combustion technology has been investigated for the next-generation coal-fired power plants (Zhigang *et al.* 2013). Thus, coal gasification with CO_2 has now emerged as a cleaner and more efficient way for the production of energy, which offers the advantages of CO_2 mitigation policies.

However, the implementation of coal gasification with CO_2 in a coal-fired power generation requires further understanding of the thermo-chemical characteristics in the process of oxidation, combustion and gasification of coal with gradual increase in the temperature in CO_2. On the other hand, understanding of the reaction behaviour of coal gasification in a CO_2 atmosphere is also essential for coal seam underground coal gasification (UCG) projects. Thus, the investigation of coal gasification and combustion reactivity with a CO_2 atmosphere will be an essential feature to allow the understanding of the reaction mechanism and kinetics for the development of the gasification technology. The CO_2 gasification study on coal, biomass and other carbonaceous materials has been extensively investigated using thermogravimetric analysis (TGA) (Ergun 1956; Zhang *et al.* 2006; Sawettaporn *et al.* 2009; Kim *et al.* 2011; Ng *et al.* 2011; Yuan *et al.* 2011; Lahijani *et al.* 2012; Jing *et al.* 2013; Kuznetsov *et al.* 2013; Skodras 2013; Wei *et al.* 2014). However, the CO_2 gasification data of Indian coals is found to be limited and in need of urgent attention (Saha *et al.* 2012; Sahu 2013; Mishra *et al.* 2014; Aranda *et al.* 2016).

In India, coals can generally be found in two main geological horizons: Gondwana sediments (Permian) and early Tertiary sediments (Eocene). The majority of the deposits (about 99%) belongs to the first category, and are located in the eastern and south-eastern parts of the country, specifically in Andhra Pradesh, Assam, and Bihar (although in very small quantities in latter two regions), Chhattisgarh, Jharkhand, Madhya Pradesh, Maharashtra, Orissa, Sikkim, Uttar Pradesh, and West Bengal. The Tertiary coalfields are mainly located in Arunachal Pradesh, Assam, Meghalaya, Nagaland, and other north-eastern regions (NER) of India and the physico-chemical characteristics and behaviour are not commensurate with the properties adopted for rank classification (Iyengar *et al.* 1960; Saikia *et al.* 2014a; Das *et al.* 2015); however, they can be mostly classified as sub-bituminous in rank. The NER Tertiary coals have high-sulphur contents (2–8%), where 75–90% is organically bound while the rest is in the inorganic form, viz., as sulphate, sulphur and pyritic sulphur (Baruah and Khare 2007). Thus, the quality/grade of these NER Indian coals is low and needs proper beneficiation. These tertiary coalfields of the north-eastern region of India are a vital source of energy and play an important role in the economic growth of the region as well as of the nation. The total reserves of these coals are estimated to be approximately 1100 Mt, which is 0.37% of India's total coal resources (Saikia *et al.* 2014a).

Zhigang *et al.* (2013) reported that the traditional coal-fired boilers use air for combustion in which N_2 gas is 79% in volume ratio. Its flue gas includes only about 15% CO_2; therefore, the CO_2 capture efficiency by post-combustion system is not high. Furthermore, CO_2 capture cost from the flue gas using amine scrubbing is expected to be relatively high. The major disadvantage of the oxygen-blown gasifier is to build an oxygen plant. In general, an oxygen plant consumes about 5% of the gross power generated, which is the main reason why the total of plant investment for an oxygen-blown plant is somewhat higher than that of an air-blown plant. As an alternative, a zero-emission power plant of pulverised coal-fired power generation in a nitrogen-free atmosphere, most known as oxy-fuel or O_2/CO_2 combustion technology for pre-combustion capture, is one of the new promising methods to approach the problem of CO_2 separation and capture. In this technology, CO_2 gas substitutes the role of O_2 gas to improve and stimulate coal conversion and reduce O_2 consumption.

The studies on the gasification behaviour of the low-quality coals are quite limited as per the best of our literature survey. Therefore, considering all these factors, a feasibility study of gasification of NER coals in a CO_2 atmosphere using thermogravimetric analysis (TGA-DTA) has been carried out. Thermogravimetric analysis (TGA-DTA) is a widely used technique to study gasification process due to its simplicity and accurate measurements (Saha *et al.* 2012). In the present study, the focus is on the thermo-chemical aspects of some low-quality NER Indian coal samples in CO_2 atmosphere, and also to evaluate the effect of coal properties on gasification reactivity. These results generated will be useful in formulating the gasification technology not only for NER coals but also for other low-quality coals of the world.

2. Materials and methods

2.1 *Coal samples*

Approximately 100 kg of each representative coal sample was collected from the Tipong and Tirap

collieries of Makum coalfield and Bapung coalfield located in the north-eastern region of India. These coal samples were obtained from 20 m coal seams and their geology was described elsewhere (Ahmed 1996; Behera 2007). The bulk samples were then reduced to 1 kg by the coning and quartering method. The coal samples were further ground (first in an impact mill and after in a mortar) and sieved, and particles of 0.211–0.053 mm were chosen for subsequent analysis.

2.2 *Physico-chemical, petrography, ash and ash-fusion temperature analyses*

The proximate analysis, total sulphur, calorific value, and ultimate analysis of the coal samples were carried out by using a Leco TGA701 Thermogravimetric Analyzer (ASTM 2011a, b, c), Leco S-144DR Dual Range Sulphur Analyzer (accuracy ±0.02) (ASTM D5016-08e1 2015), Leco AC-350 Automatic Bomb Calorimeter (ASTM 2011a, b, c), and Truspec CHN Macro Determinator (630–100–300) (ASTM D3176-15 2015).

Petrographic analysis of the coal samples and identification of maceral types were performed according to standard procedures, where the coal samples were crushed to obtain a ∼18 mesh (<1 mm) size fraction to prepare polished mounds or pellets. A mixture of hardener and Canada wax or coal mounting resin in the ratio 1:5 was used for embedding the coal samples for pellet preparation, followed by their grinding and polishing. Microscopic observation has been made in a Leica DMLP microscope under both white incident light as well as fluorescence mode. The microscope is provided with 10× ocular and 10× dry lens objective. Recommendations of Stach *et al.* (1982) and ICCP have been followed for data collection and their interpretation. The volume percentages of various macerals were calculated using a swift point counter (Stach *et al.* 1982).

The ash analyses (ash chemistry) of the coal samples were carried out by using standard methods reported in the literature (Himus 1954; Jeffery *et al.* 1989). The ash fusion temperature (AFT) measurements were determined by using an ash fusion point determination apparatus (Leitz Wetzlar). It was carried out by heating a little amount of coal ash sample (∼2 mg) at a rate of 10°C min^{-1} up to 1000°C, and then changing the heating rate to 5°C min^{-1} up to 1600°C in the absence of air. During the process, the initial deformation temperature (IDT), hemispherical temperature (HT) and final fusion temperature (FT) were recorded according to the specific shapes of the ash cylinder formed.

2.3 *Fourier Transform Infrared (FT-IR) spectroscopic and X-ray diffraction analysis (XRD)*

The XRD analysis was used for the qualitative assessment of the minerals present in the coal samples. FTIR spectra were recorded to investigate the surface functional groups and the type of chemical bonding environment in the coal samples.

The FT-IR spectra of the coal samples were recorded on a Perkin–Elmer system 2000 (model 640B, software version 4.07) using a KBr pellet. The XRD analysis of the coal samples was performed in X-ray Diffractometer (Rigako, ULTIMA IV). X-ray diffraction data were obtained with the start angle 5.00, stop angle 100.00 and step angle 0.02° with a scanning rate of 4° per minute and target Cu K α ($\lambda = 1.54056$ Å). The program 'XG operation RINT 2200' associated with the XRD was used to process the diffractogram and the library database 'Rigaku PDXL 1.2.0.1' was used for identification of the peaks.

2.4 *Thermogravimetric analysis-differential thermal calorimetry (TGA-DTA)*

Non-isothermal thermogravimetric analysis (TGA-DTA) of the coal samples was performed in a thermal analyser (Netzsch STA 449F3 Jupiter) to study the gasification of the coal samples with CO_2. The experiments were carried out with a heating rate of 10, 15 and 20°C min^{-1} from room temperature to 1400°C using an Al_2O_3 crucible under CO_2 (60 ml min^{-1}) atmosphere. The termination temperature of the experimental run was set up to 1400°C in order to reduce the unburned carbon content. Approximately 30 mg of the sample was used for each experimental run, and duplicate experiments were also carried out for each of the samples. Similarly, the isothermal TGA-DTA of the coal samples were carried out by taking ∼30 mg of the samples and heating at 30°C min^{-1} to 1000°C, under N_2 (50 ml min^{-1}). Samples were then maintained at 1000°C with the replacement of N_2 by CO_2 (50 ml min^{-1}) for $1\frac{1}{2}$ hrs to determine the isothermal reactivity test.

The temperature calibration was done at a heating rate of 10, 15 and 20°C min^{-1} by analysing the TGA-DTA signal of the melting peak (Tm) of the pure substances In (Tm = 431.8 K), Al (Tm = 959.2 K), Au (Tm = 1346.9 K), Sn (Tm=508.4 K), and Zn (Tm = 700.8 K) using the same crucibles (Al_2O_3) and similar conditions. Accordingly, a baseline correction was also done in a CO_2 environment at a heating rate of 10, 15 and 20°C min^{-1} from room temperature to 1400°C using an Al_2O_3 crucible.

2.5 *Model-free kinetics and data processing*

The Netzsch Thermokinetics 3.1 (version 072010) was used for processing of the non-isothermal TGA data (Budrugeac 2013). The activation energies (E), which depend on the degree of conversion (α) were evaluated by this software package, which allowed the evaluation of the dependence of E on α by means of Freidman model-free methods.

2.5.1 *Friedman method (FR)*

It is a differential isoconversional method, which calculates the reaction parameters without any presumption about the kinetic model or reaction types and is directly based on the Arrhenius equation (equations 1 and 2) (Budrugeac 2013).

$$\frac{d\alpha}{dt} = k(T) f(\alpha)\,, \tag{1}$$

$$k\,(T) = A \exp\left(-\frac{E}{RT}\right). \tag{2}$$

Here, $f(\alpha)$ is a function describing the hypothetical model of a reaction mechanism, k is the reaction rate, A is the pre-exponential factor, E is the activation energy, R is the gas constant (8.314 J $K^{-1}mol^{-1}$), T is the absolute temperature, t is the time and α is the loss in mass or mass conversion ratio.

For the non-isothermal experiments (with a linear heating rate,) equation (1) can be written as:

$$\frac{d\alpha}{dT} = \frac{A}{\beta} \exp\left(\frac{-E}{RT}\right) f(\alpha)$$

or

$$\frac{d\alpha}{f(\alpha)} = \frac{A}{\beta} \exp\left(\frac{-E}{RT}\right) dT, \tag{3}$$

where, the term $d\alpha/dt$ is known as the rate of the reaction at non-isothermal conditions.

The logarithm of equation (3) can be written as:

$$\ln \frac{d\alpha}{dt} = \ln\left(\beta \frac{d\alpha}{dT}\right) = \ln\left[A f(\alpha)\right] - \frac{E}{RT}. \tag{4}$$

From the above equation of Friedman method, it is easy to obtain values for the activation energy over a wide range conversions by plotting $\ln\left(\beta \frac{d\alpha}{dT}\right)$ *vs.* $\frac{1}{T}$ for a constant α value. The method gives the activation energy value depending on conversion of α.

3. Results and discussion

3.1 *Physico-chemical, petrography, ash and ash-fusion temperature characteristics*

The physico-chemical and petrographic characteristics (mmf) of the coal samples are summarised in table 1. The moisture and volatile matter content of the coals vary from 2.35 to 2.70% and 36.90 to

Table 1. *Physico-chemical, petrographic properties of the three coals (as received basis, wt%).*

	Coal samples		
Parameter	Tirap	Tipong	Bapung
Proximate analysis (wt%)			
Moisture	2.70	2.40	2.35
Ash	3.90	3.68	11.50
Volatile matter	41.20	42.80	36.90
Fixed carbon	52.20	52.40	49.25
Ultimate analysis (%)			
Carbon	69.90 (74.83)	76.10 (81.02)	73.23 (85.00)
Hydrogen	4.80 (5.13)	5.41 (5.76)	5.00 (5.80)
Nitrogen	1.30 (1.39)	1.24 (1.32)	1.36 (1.57)
Oxygen (by difference)	21.50 (18.65)	16.07 (11.90)	15.95 (7.63)
Others			
Total sulphur (%)	2.50	1.18	4.46
Gross calorific value (Kcal kg^{-1})	7340	7760	6190
Net calorific value (Kcal kg^{-1})	7312	7735	6166
Petrographic properties: Maceral analysis (vol.%, m.m.f)			
Vitrinite	85.40	83.40	78.40
Liptinite	9.70	12.30	8.40
Inertinite	4.90	4.30	13.20

The values within bracket are 'in dry and ash free basis (d.a.f.)'.

42.80%, respectively. The coals are of low ash yield (3.68–11.5%). The carbon content (on dmf basis) indicates that the coals are sub-bituminous to low-rank bituminous. The petrographic analysis shows that the coal samples are high in vitrinite content (78.4–85.4%). The Tipong coal sample contains higher liptinite than the other two samples, whereas the Bapung coal has higher inertinite content than the others. Vitrinite and liptinite are reactive towards gasification, whereas inertinite is composed of condensed aromatic nuclei, densest, and less reactive (Sharma *et al.* 2012; Gomes *et al.* 2006).

The ash chemistry and the ash fusion temperature ranges are reported in table 2. The acidic quality of the coal-ashes is dominated by SiO_2 and Al_2O_3 reflecting the high contributions of the quartz and clay minerals (see table 3, figure 1). The total alkali content (Na_2O+K_2O) of Tipong coal (1.58%) is found to be high in comparison to Tirap coal (1.14%), followed by Bapung coal (0.56%). The presence of high alkali content could enhance the reactivity towards the oxidising gases including CO_2.

The ash fusion temperature (AFT) ranges, depending upon the chemical composition of coal ash, are used for understanding the fusion behaviour of the coal ashes. In the present study, the observations are mostly made considering the initial deformation temperature (IDT), where most of the melting takes place in this temperature range and therefore low ash fusion temperatures are observed (see table 2). The initial deformation (ID) temperature of the three coal ash is found to be in the range 1100°–1210°C.

3.2 *X-ray diffraction (XRD) and Fourier Transform Infrared (FT-IR) spectroscopic analyses*

The X-ray diffractograms of the coal samples are shown in figure 1. The qualitative assessment of the XRD d-values was carried out to determine the presence of minerals in the coal samples with the help of the literature available elsewhere (Saikia *et al.* 2009, 2014b) (table 3). The major minerals present in the samples are gypsum (G), hematite (H), quartz (Q), muscovite (M), illite (I), pyrite (Py), marcasite (M) and kaolinite (K). Figure 2 shows the FT-IR spectra of the coal samples, and the assignments of the functional groups from their stretching frequencies are summarised in table 4. The FT-IR spectra are

Table 2. *Ash and ash fusion temperature analysis, slagging potential, alkali index and Fouling potential of the three coals.*

Parameter	Coal samples		
	Tirap	Tipong	Bapung
Ash analysis (%)			
Ash	3.51	3.68	11.50
SiO_2	47.80	45.80	50.33
Fe_2O_3	28.80	18.30	8.41
Al_2O_3	25.90	27.80	37.54
CaO	0.92	1.02	0.54
MgO	0.13	0.86	0.31
TiO_2	1.02	1.05	1.53
Na_2O	0.34	0.38	0.50
K_2O	0.80	1.20	0.06
Base/Acid ratio	0.41	0.30	0.24
Slagging potential			
Fe_2O_3/CaO	31.30	17.94	15.60
SiO_2/SiFeCaMg	0.62	0.70	0.77
Slagging factor (Base/Acid) × (S dry)	1.30	0.34	1.09
Fouling potential			
Fouling factor (Base/Acid) × (Na_2O+K_2O)	0.47	0.33	0.80
Abrasion potential (SiO_2/Al_2O_3)	1.85	1.65	1.34
Alkali index	1.48	1.20	2.85
Ash fusion temperature (°C)			
Initial deformation temperature (IDT)	1100	1210	1180
Hemispherical temperature (HT)	1240	1360	1360
Formation temperature (FT)	1500	1460	>1500

Base = $Fe_2O_3+CaO+MgO+K_2O+Na_2O$. Acid=$SiO_2+TiO_2+Al_2O_3$.
Alkali index = Ash (%)*($Fe_2O_3+CaO+MgO+K_2O+Na_2O$/ $SiO_2+Al_2O_3$)·
SiFeCaMg = $SiO_2+Fe_2O_3+CaO+MgO$.

Table 3. *Assignment of d-values in XRD of coal samples.*

Coal samples	d-values	Assignments
Tirap	7.20	Gypsum (G), Kaolinite (K)
	4.27	Gypsum (G)
	3.35	Quartz (Q)
Bapung	7.26	Gypsum (G), Kaolinite (K)
	4.90	Quartz (Q)
	4.28	Quartz (Q)
	3.59	Quartz (Q), Illite (I), Hematite (H)
	3.37	Quartz (Q), Illite (I)
	1.82	Quartz, Hematite, Pyrite, Marcasite
Tipong	3.35	Quartz
	2.13	Quartz
	1.88	Hematite, Quartz, Marcasite
	1.54	Hematite, Quartz
	1.37	Hematite, Quartz

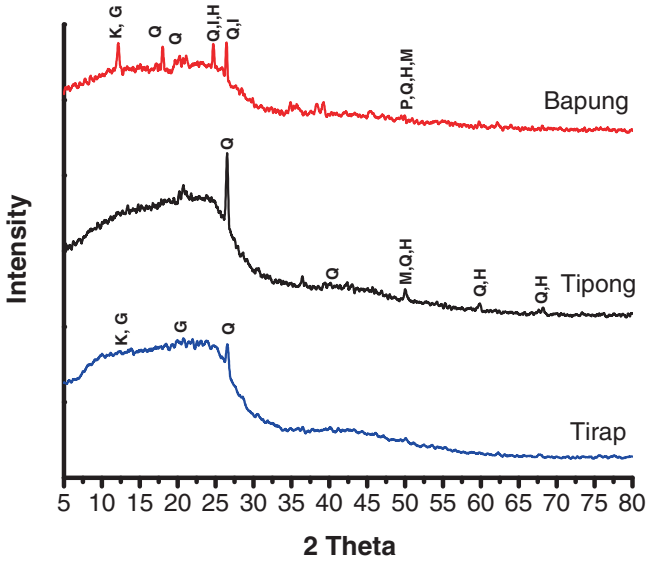

Figure 1. XRD of the coal samples.

observed to be similar in nature for all the three coal samples.

3.3 *Thermogravimetric (TGA-DTA) analysis CO_2 gasification of coal*

Figure 3 shows the thermogravimetric-differential thermogravimetry (TGA-DTG) and differential thermal analysis (TGA-DTA) patterns of non-isothermal CO_2 gasification of the coal samples. The thermal changes observed can be divided into four temperature stages. Weight loss is observed in the temperature regions between 25°–100°C and 108°–276°C, which are due to the calefactive-evaporated-alleviative (water loss) and calefactive-adsorption-weight incremental (CO_2 absorption) processes, respectively (Zhigang *et al.* 2013). At temperature range 276°–650°C, calefactive-devolatilization-alleviative process (primary and secondary devolatilization) takes place during the thermal process (Zhigang *et al.* 2013). Over 650°C, calefactive-char formation and the gasification-alleviative process take place (Zhigang *et al.* 2013), and the maximum weight loss is calculated to be about 48.59%, 61.01% and 56.22% for Tirap, Tipong, and Bapung coal samples, respectively. The maximum gasification temperature (corresponding to the maximum weight loss in DTG) is found to be ≥1100°C for all the three coal samples. The reaction between coal and CO_2 is an endothermic process and occurs at higher temperature ranges 1100°–1400°C, which is also supported by the DTA endothermic peaks that appear at around 1100°–1300°C for the sample spectra (Zhigang *et al.* 2013) (see figure 3a–i). Thus, the present study shows that the coal gasification of low-quality NER coals with CO_2 mainly occurs in the temperature range of 800°–1400°C and is a maximum at around 1100°C. The results are found to be in accordance with the results reported elsewhere (Jing *et al.* 2013; Zhigang *et al.* 2013).

The role of mass transfer phenomena is also experimentally verified by comparing the TGA-DTG plots for the same material but at different flow rates (for external diffusion) (figure 4a). It is observed that external diffusion cannot take place in the gasification process, but internal diffusion may take place during the gasification process since the mass loss is dependent on the rate of heating, sample mass and size of the particles (figure 4b). However, in the present study, it is ignored and will be discussed in our future works.

3.4 *Determination of the activation energy of the CO_2 gasification process*

The non-isothermal kinetics of mass loss during the gasification of coal samples in a CO_2 environment

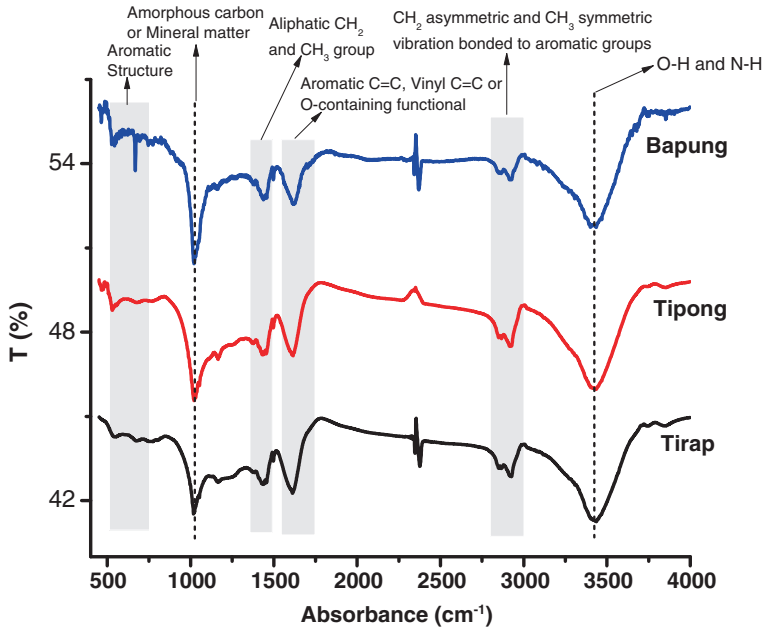

Figure 2. FT-IR spectra of coal samples.

Table 4. *Assignments of the FT-IR peaks of the samples.*

Samples	Wave number (cm^{-1})	Assignments
Tirap	3435.7 (b)	O–H and N–H stretching vibrations
	2926.2 (m) 2866.29 (w) 2855.0 (w)	CH_2 asymmetric vibration and CH_3 symmetric vibration bonded to aromatic groups
	1611.5 (s)	Aromatic C=C stretching vibrations, Vinyl C=C or other O-containing functional groups
	1498.0 (m) 1433.3 (m)	Aliphatic CH_2 and CH_3 groups
	1162.7 (s, b) 1011.1 (w)	Amorphous carbon or mineral matter
	800–530 (m)	Aromatic structures
Tipong	3435.5 (b)	O–H and N–H stretching vibrations
	2850.0 (m) 2877.3 (w) 2922.7 (w)	CH_2 asymmetric vibration and CH_3 symmetric vibration bonded to aromatic groups
	1614.9 (s)	Aromatic C=C stretching vibrations, Vinyl C=C or other O-containing functional groups
	1429.4 (m)	Aliphatic CH_2 and CH_3 groups
	1162.7 (s, b) 1133.5 (w)	Amorphous carbon or mineral matter
	800–530 (m)	Aromatic structures
Bapung	3435.5 (b)	O–H and N–H stretching vibrations
	2850.0 (m) 2870.3 (w) 2922.7 (w)	CH_2 asymmetric vibration and CH_3 symmetric vibration bonded to aromatic groups
	1614.9 (s)	Aromatic C=C stretching vibrations, Vinyl C=C or other O-containing functional groups
	1429.4 (m)	Aliphatic CH_2 and CH_3 groups
	1162.7 (s, b) 1133.5 (w)	Amorphous carbon or mineral matter
	800–530 (m)	Aromatic structures

Note. w: weak; m: medium; s: strong; b: broad.

at a temperature range of 800°–1400°C was evaluated by using the Freidman methods with the help of the thermokinetic software associated with the instrument. The results are summarised in table 5. Figure 5(a–c) shows the Freidman (FR) analysis of the samples, which shows the variation of $\ln(d\alpha/dt))$ with $1/T$. The activation energy (E) can be calculated for each degree of conversion (α) from the slope (E/R) of the straight line obtained. Figure 5(d–f) shows the corresponding activation

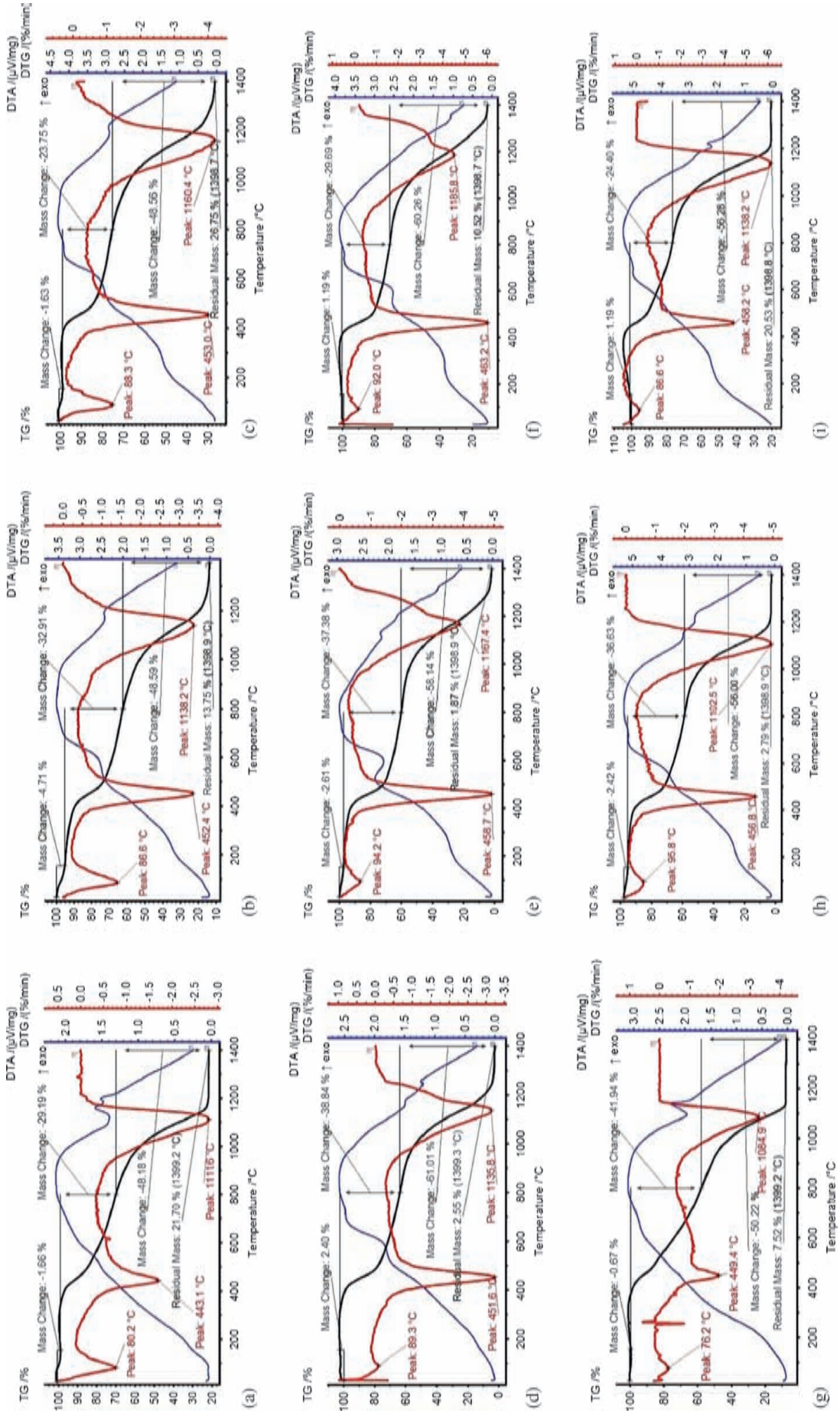

Figure 3. TGA-DTA of Bapung (**a**, **b**, **c**), Tipong (**d**, **e**, **f**) and Tirap (**g**, **h**, **i**) at CO_2 environment (a, d, e at 10°C/min; b, e, f at 15°C/min; and c, f, i at 20°C/min).

energy (E) plots of the Freidman analysis and the three stages with different activation energies can be obtained for each of the samples.

3.5 *Application of multivariate non-linear regression analysis*

The results obtained by the FR methods show that the gasification of the coal samples in a CO_2 environment is a complex process (figure 5a–f).

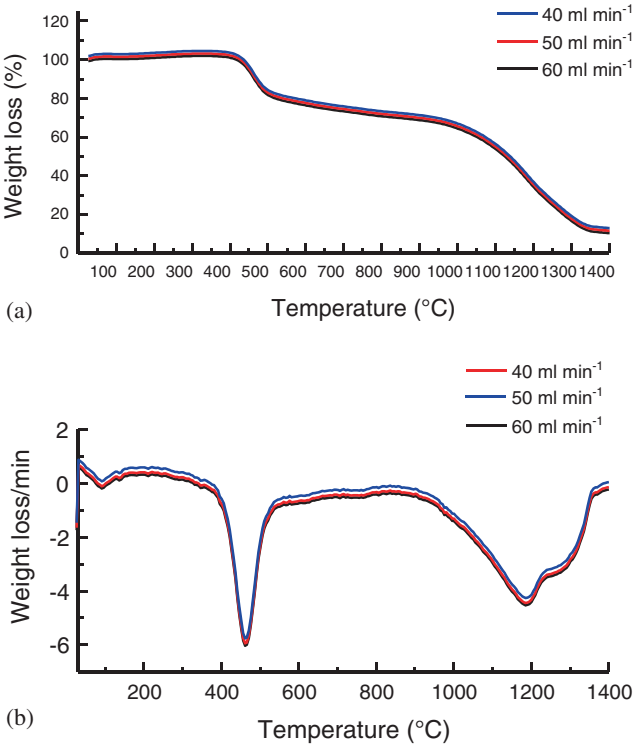

Figure 4. TGA-DTG plots of the Tirap coal sample at different flow rates (for external diffusion).

Thus, a multivariate non-linear regression analysis was performed by using the thermokinetic software to find out the mechanisms, formal reaction model, and the corresponding kinetic triplets of coal gasification in a CO_2 atmosphere. The calculations were done by considering many reaction models associated with the software.

The analysis of the non-isothermal data and F-test fit quality of the samples shows that the coal gasification is satisfactorily described by the kinetic models of nth order with autocatalysis by B for the Tirap, and Bapung coal samples and an nth order for the Tipong coal sample. The corresponding kinetic parameters are listed in table 5. Finally, after multivariate non-linear regression analysis, the activation energies (E) and pre-exponential factors (A) of the processes for the Tirap, Tipong, and Bapung coal samples were found to be 135.20 kJ mol^{-1}, 146.81 kJ mol^{-1}, 129.07 kJ mol^{-1} and 1.29×10^2 s^{-1}, 8.06×10^2 s^{-1}, and 1.17×10^2 s^{-1}, respectively.

Thus, the possible kinetic rate equations for CO_2 gasification of these low-quality coal samples can be described as follows:

- The Tirap coal (equation 5) and Bapung coal (equation 6) samples follow the single step ($A\longrightarrow B$) nth order with autocatalysis, where the order of the reaction (n) was found to be 0.96681 and 0.85627, respectively (table 5):

$$\frac{d\alpha}{dt} = 1.29\times10^2 e^{-135.20/RT} f(\alpha) \qquad (5)$$

$$\frac{d\alpha}{dt} = 1.17\times10^2 e^{-129.07/RT} f(\alpha) \qquad (6)$$

- The Tipong coal sample follows the single step ($A\longrightarrow B$), nth order reaction, where the order

Table 5. *Kinetic and statistical parameters of the coal gasification in CO_2 atmosphere.*

Kinetic models			
	Value		
	Tirap coal	Tipong coal	Bapung coal
Kinetic parameters			
Model step	nth order with autocatalysis by B	nth order	nth order with autocatalysis by B
log (A1/s^{-1})	2.11062	2.90684	2.07001
E (kJ mol^{-1})	135.20	146.81	129.00
Reaction order	0.96681	0.46376	0.85627
Statistical parameters			
Least squares	9828.60954	11798.08518	13807.32981
Mean of residues	5.22510	5.72472	6.19304
Max. no. of cycles	50	50	50
Number of cycles	18	2	2
Correlation coefficient	0.999355	0.999161	0.998668
Rel. precision	0.001000	0.001000	0.001000
Durbin–Watson value	0.009	0.010	0.011
Durbin–Watson factor	10.609	10.095	9.650

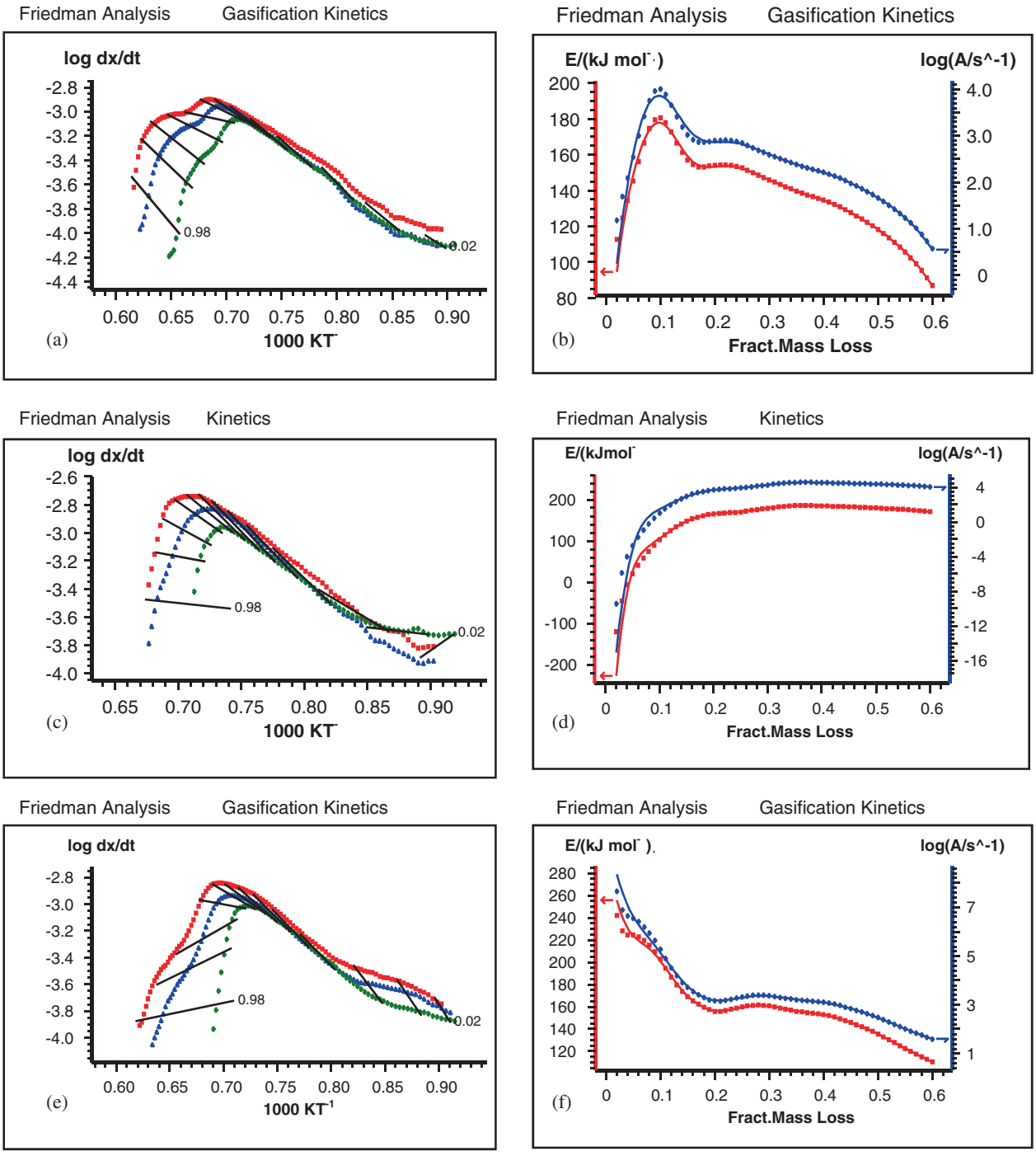

Figure 5. Freidman analysis and corresponding energy plot diagram of the Tirap **(a**, **b)**, Tipong (**c**, **d**) and Bapung **(e**, **f)** samples.

of the reaction (n) is found to be 0.46376 (table 5):

$$\frac{d\alpha}{dt} = 8.06 \times 10^2 e^{-146.81/RT} f(\alpha)\,.$$

3.6 *CO_2 gasification reactivity of the coal samples*

Figure 6 depicts the isothermal reactivity of the CO_2 gasification of the low-quality coal samples. The reactivity of the coal samples in isothermal conditions was calculated using the methods reported elsewhere (Takayuki *et al.* 1985; ASTM D3176-15; ISO/CD 18894 2006; Machado *et al.* 2010; Ng *et al.* 2011; Huo *et al.* 2014). It demonstrates that the reactivity of CO_2 gasification of the coal samples can be ranked as Bapung coal<Tirap coal<Tipong coal. Figure 6 can also be used for the graphical evaluation of the isothermal thermogravimetric analysis of the samples. Point 1 indicates the effect of buoyancy force of the beginning

of the test and point 2 is the beginning of the pyrolysis. Point 3 indicates the beginning of the gasification reaction to the injection of CO_2 and point 4 is the reaction region between carbon particles and CO_2. Table 6 presents the values of the reactivity measurements from the isothermal thermogravimetric analysis. The Tipong coal sample has the highest reactivity and it reacts with CO_2 faster than the Tirap and Bapung coal samples. The time to reach a maximum reaction rate for the Tirap coal samples was found to be highest in comparison to the Tipong and Bapung coal samples. The time required to reach the point of 50% of carbon conversion for the Bapung and Tirap coal samples are around 52.75 and 41.50 minutes, respectively, whereas, for the Tipong coal sample, the time required is considerably less (around 24.75 minutes). Thus, the thermogravimetric technique may be considered as a potential tool to understand the CO_2 gasification of low-quality coals.

The reactivity index, $R_{0.5}$ ($R_{0.5}$=0.5/t_{50}) is a way to express the reactivity of the coal samples during gasification (Huo *et al.* 2014), where, t_{50} is the time for 50% of carbon conversion. The reactivity index of the Tirap, Tipong and Bapung coal samples were found to be 0.0120, 0.0204, and 0.0094 min^{-1}, respectively. Thus, the reactivity index of the Tipong coal sample is higher than that of the Tirap and Bapung coal samples and the reactivity of the coal samples towards

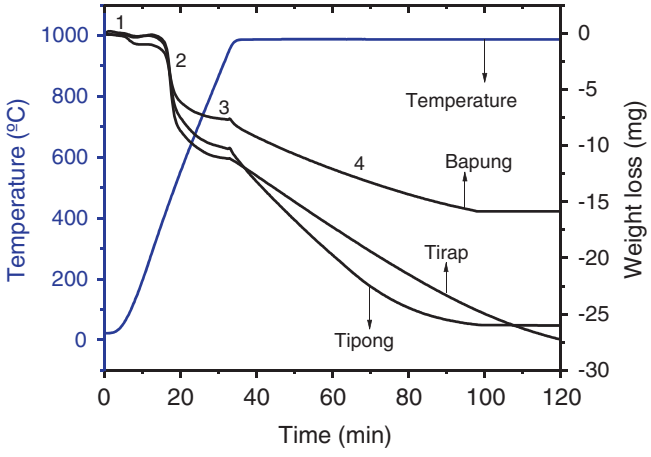

Figure 6. Isothermal analysis of the coal samples for their reactivity measurement.

CO_2 can be ranked as Bapung coal<Tirap coal<Tipong coal.

3.7 *Factors affecting the activation energy and reactivity of CO_2 gasification*

The activation energy of the coal samples for CO_2 gasification can be ranked as Bapung coal<Tirap coal<Tipong coal. It indicates that the sensitivity of the gasification rate to gasification temperature of Bapung coal is weaker than that of Tirap and Tipong coals. The activation energy of Bapung coal is the lowest and this may be due to the highest alkali index (2.48). It was reported that the alkali and alkaline earth metal (Na_2CO_3, KCl, NaCl, $CaCl_2$, CaO) and metal species such as Mg, Ba, Fe, Ni, Mn can catalyse the gasification reaction and lower the activation energy (Kuznetsov *et al.* 2013). Also the catalysts like $Fe(NO_3)_3$, $FeCl_3$, K_2CO_3 decreases the activation energy of a gasification process (Veraa and Bell 1978; Lahijani *et al.* 2012; Zhou *et al.* 2012).

On the other hand, the reactivity of carbonaceous materials towards CO_2 depends on the volatile matter, mineral matter, carbon content, petrography and structure of the materials (Takayuki *et al.* 1985; ASTM D3176-15; ISO/CD 18894 2006; Ng *et al.* 2011; Machado *et al.* 2010; Huo *et al.* 2014). However, in the present study, volatile matter may not be the main factor affecting the reactivity of the samples, since almost all of the volatile matter is removed during the pyrolysis step (figure 3). Thus, the structure of the samples, petrography and ash content may play a major role in the reactivity. The reactivity of the Tipong coal is found to be highest, which may be due to its high vitrinite and liptinite content (table 1). The alkali index sequence for the samples can be ranked as Bapung coal<Tirap coal<Tipong coal. There is no good relationship observed between the reactivity and alkali index for the coal samples in this study. The reactivity of the Bapung coal (ash yield: 11.5%) is found to be lower compared to the Tirap (ash yield: 3.90%) and Tipong coal (ash yield: 3.68%), which may be due to the localised deposition of metal particles on the char surface and forming clusters. High concentrations of metal-imposed inhibitions are either by blocking

Table 6. *Calculated isothermal thermogravimetric analysis values for reactivity measurement at 1000° C.*

Coal samples	Experimental maximum reaction rate (mg/min^{-1})	Time to reach the maximum reaction rate (min)	Time to reach 50% conversion (min)	Reactivity at maximum reaction rate (min^{-1})	Reactivity index ($R_{0.5}$) (min^{-1})
Tirap	9.99	74.25	41.50	0.54	0.0120
Tipong	9.99	45.75	24.50	0.62	0.0204
Bapung	9.95	39.75	52.75	0.70	0.0094

of accessible active sites on the char surface or deactivation of neighbouring alkali due to the formation of agglomerate (Lahijani *et al.* 2012). It was also reported that the catalytic metals such as Ca, K, and Na lose their activity by the formation of the stable aluminosilicate or through vapourisation (Saha *et al.* 2012). After replacement of N_2 by CO_2 at a temperature of 1000°C for reactivity measurement at the isothermal condition, the rearrangement of the carbon structure takes place and less amount of active sites are available on coal surface.

4. Conclusions

From our study, it may be concluded that CO_2 gasification of the low-quality coals at higher temperature mainly occurs at the temperature range of 800°–1400°C and is maximum at around 1100°C. The CO_2 gasification kinetics of low-quality Indian coals at the temperature range of 800°–1400°C in a CO_2 environment follows the '*n*th order with autocatalysis (CnB)' and '*n*th order (Fn)' mechanism. The activation energy of the CO_2 gasification of the low-quality Indian coal samples is observed to be in the range of 129.07–146.81 kJ/mol. It is observed that the Tipong coal is the most suitable among these three low-quality coals for gasification under a CO_2 environment. However, the effect of structural parameters such as pore structure (meso and micropore), surface area, catalytical effect of alkali and alkaline earth metal, flue gas analysis and effect of CO_2 on syngas during on CO_2 gasification of the low-quality coals is to be studied further. Also, the changes occurred after gasification of the samples is to be studied.

Acknowledgements

The authors express their thanks to the Director of CSIR-NEIST, Jorhat, for his continuous encouragement. The authors are grateful to CSIR, New Delhi (MLP-6000-WP-III) and Department of Information Technology, Govt. of India (GAP-0261) for financial support. The suggestions received from Dr B P Baruah are thankfully acknowledged. Special thanks are given to all the staff of Coal Chemistry Pilot Plant (CSIR-NEIST) for their assistance during the study. The authors appreciate the esteemed reviewers for their constructive comments to improve the paper.

References

Ahmed M 1996 Petrology of Oligocene coal, Makum coalfield, Assam, northeast India; *Int. J. Coal Geol.* **30** 319–325.

ASTM 2011a *Test Method for Moisture in the Analysis Sample of Coal and Coke*; ASTM International, West Conshohocken, PA.

ASTM 2011b Annual book of ASTM standards. *Test Method for Ash in the Analysis Sample of Coal and Coke*; ASTM International, West Conshohocken, PA.

ASTM 2011c *Test Method for Volatile Matter in the Analysis Sample of Coal and Coke*; ASTM International, West Conshohocken, PA.

ASTM D3176-15 2015 West Conshohocken PA. http://www.astm.org.

ASTM D5016-08e1 2015 West Conshohocken PA. http://www.astm.org.

Aranda G, Grootjes A J, van der Meijden C M, van der Drift A, Gupta D F, Sonde R R, Poojari S and Mitra C B 2016 Conversion of high-ash coal under steam and CO_2 gasification conditions; *Fuel Process. Technol.* **141(1)** 16–30.

Baruah B P and Khare P 2007 Desulphurization of oxidized Indian coals with solvent extraction and alkali treatment; *Energy and Fuels* **21** 2156–2164.

Behera P 2007 Volatile displacement of Meghalaya coals – A pointer to explore low sulphur coals; *J. Earth Syst. Sci.* **116** 137–142.

Budrugeac P 2013 Thermokinetic study of the thermooxidative degradation of a composite epoxy resin material; *Rev. Roum. Chim.* **58(4–5)** 371–379.

Das T, Saikia B K and Baruah B P 2015 Formation of carbon nano-balls and carbon nano-tubes from northeast Indian Tertiary coal: Value added products from low-quality coal; *Gondwana Res.* **31** 295–304.

Ergun S 1956 Kinetics of the reaction of carbon with carbon dioxide; *J. Phys. Chem.* **60(4)** 480–485.

Gomes M L I, Osorio E and Vilela A C F 2006 Thermal analysis evaluation of the reactivity of the mixture for injection in the blast furnace; *Mat. Res.* **9(1)** 91–95, doi: 10.1590/S1516-14392006000100017.

Himus W G 1954 *Fuel testing laboratory methods in fuel technology*; A text book; University Press, Aberdeen, Great Britain.

Huo W, Zhou Z, Chen X, Dai Z and Yu G 2014 Study on CO_2 gasification reactivity and physical characteristics of biomass, petroleum coke and coal chars; *Bioresource Technol.* **159** 143–149.

Irfan M F, Usman M R and Kusakabe K 2011 Coal gasification in CO_2 atmosphere and its kinetics since 1984: A brief review; *Energy* **36** 12–40.

ISO/CD 18894 2006 Coke-determination of coke reactivity index (CRI) and coke strength after reaction (CSR).

Iyengar M S, Guha S and Beri M L 1960 The nature of sulphur groupings in abnormal coals; *Fuel* **39** 235–243.

Jeffery G H, Bassett J, Mendham J and Denny R C 1989 *Vogel's textbook of quantitative inorganic chemistry*; 5th edn.

Jing X, Wang Z, Zhang Q, Yu Z, Li C, Huang J and Fang Y 2013 Evaluation of CO_2 gasification reactivity of different coal rank chars by physico-chemical properties; *Energy and Fuels* **27** 7287–7293.

Kim Y T, Seo D and Hwang J 2011 Study of the effect of coal type and particle size on char–CO_2 gasification via gas analysis; *Energy and Fuels* **25(11)** 5044–5055.

Kuznetsov P N, Kolesnikova S M and Kuznetsova L I 2013 Steam gasification of different brown coals catalysed by the naturally occurring calcium species; *Int. J. Clean Coal Energ.* **2** 1–11.

Lahijani P, Zainal Z A and Mohamed A R 2012 Catalytic effect of iron species on CO_2 gasification reactivity of oil palm shell char; *Thermochim. Acta* **546** 24–31.

Machado J G M S, Osorio E and Vilela A C F 2010 Reactivity of Brazillian coal and blends aiming to their injection into blast furnaces; *Mat. Res.* **13(3)** 287–292.

Mishra A, Gautam S and Sharma T 2014 Effect of char structure on coal gasification; *J. Basic Appl. Eng. Res.* **1** 1–3.

Ng K W, MacPhee J A, Giroux L and Todoschuk T 2011 Reactivity of bio-coke with CO_2; *Fuel Process. Technol.* **92** 801–804.

Saha S, Sahu G, Sharma B K and Sharma T 2012 Variation of CO_2 gasification reactivity in gravity separated coal samples; *J. Mines, Metals & Fuels* **60** 7–8.

Saha S, Sahu G, Dutta S, Chavan P, Sinha A K, Sharma B K and Sharma T 2013 Studies on CO_2 gasification reactivity of high ash Indian coal; *IJETAE* **3** 29–33.

Sahu H B 2013 Implementing clean coal technology through gasification and liquefaction – the Indian perspective; *Int. J. Chem. Tech. Res.* **5** 824–830.

Saikia B K, Goswamee R L, Baruah B P and Baruah R K 2009 Occurrence of some hazardous metals in Indian coals; *Coke Chem. USSR* **52** 54–59.

Saikia B K, Dutta A, Saikia L, Ahmed S and Baruah B P 2014a Ultrasonic assisted cleaning of high-sulphur Indian coals in water and mixed alkali; *Fuel Process. Technol.* **123** 107–113.

Saikia B K, Ward C R, Oliveira M L S, Hower J C, Baruah B P, Braga M and Silva L F 2014b Geochemistry and nano-mineralogy of two medium-sulphur northeast Indian coals; *Int. J. Coal Geol.* **121** 26–34.

Sawettaporn S, Bunyakiat K and Kitiyanan B 2009 CO_2 gasification of Thai coal chars: Kinetics and reactivity studies; *Korean J. Chem. Eng.* **26(4)** 1009–1015.

Sbirrazzuoli N, Vincent L, Mija A and Guigo N 2009 Integral differential and advance isoconversional methods. Complex mechanism and isothermal predicted conversion-time curves; *Chemomet. Intell. Lab. Syst.* **96** 219–226.

Sharma A, Saikia B K and Baruah B P 2012 Maceral contents of Tertiary Indian coals and their relationship with calorific values; *IJIRD* **1(7)** 196–203.

Sinag A, Sinek K, Tekes A T, Misirlioglu Z, Canel M and Wang L 2003 Study on CO_2 gasification reactivity of chars obtained from Soma–Isikar Lignite (Turkey) at various coking temperature; *Chem. Eng. Process.* **42** 1027–1103.

Skodras G 2013 Catalysis and compensation effect of K_2CO_3 in low-rank coal-CO_2 gasification; *Cent. Eur. J. Chem.* **11(7)** 1187–1200.

Stach E, Mackowsky M T, Teichmuller M, Taylor G H, Chandra D, Teichmuller R (eds) 1982 Stach Text book of Coal Petrology; Borntniger, Stuttgart.

Takayuki T, Hashimot K and Silveston P L 1985 Reactivities of 34 coals under steam gasification; *Fuel* **64** 1438–1442.

Veraa M J and Bell A T 1978 Effect of alkali metal catalysts on gasification of coal char; *Fuel* **57** 194–200.

Wei H, Zhijie Z, Chen X, Dai Z and Yu G 2014 Study on CO_2 gasification reactivity and physical characteristics of biomass, petroleum coke and coal chars; *Bioresource Technol.* **159** 143–149.

Yuan S, Chen X L, Li J and Wang F C 2011 CO_2 gasification kinetics of biomass char derived from high-temperature rapid pyrolysis; *Energy and Fuels* **25(5)** 2314–2321.

Zhou L, Zhang G, Schurz M, Steffen K and Meyer B 2016 Kinetic study on CO_2 gasification of brown coal and biomass chars: Reaction order; *Fuel* **173(1)** 311–319.

Zhang L X, Huang J J, Fang Y T and Wang Y 2006 Gasification reactivity and kinetics of typical Chinese anthracite chars with steam and CO_2; *Energy and Fuels* **20(3)** 1201–1210.

Zhigang Li, Zhang X, Sugai Y, Wang J and Sasaki K 2013 Measurements of gasification characteristics of coal and char in CO_2-rich gas flow by TG-DTA; *J. Combustion,* Article ID **985687** 1–15, doi: 10.1155/2013/985687.

Zhou Z, Hu Q, Liu X, Yu G and Wang F 2012 Effect of iron species and calcium hydroxide on high-sulphur petroleum coke CO_2 gasification; *Energy and Fuels* **26** 1489–1495.

MS received 7 December 2015; revised 30 May 2016; accepted 8 June 2016

Corresponding editor: N V Chalapathi Rao